International Research Journal of Engineering and Technology (IRJET) e-ISSN: 2395-0056
Volume: 11 Issue: 05 | May 2024 www.irjet.net p-ISSN: 2395-0072

# Axial Compression Behavior of 3D Printed Bioinspired Honeycomb Structures Fabricated from MWCNT-Reinforced PETG Polymer Composites

**Shaik Firoz Basha[1], N Phani Raja Rao[2]**

*[1]M.Tech Student, Production Engineering Dept & Sri Venkateswara Institute of Technology, N.H 44, Hampapuram, Rapthadu, Andhra Pradesh, India*
*[2]Associate Professor and HOD, Production Engineering Dept & Sri Venkateswara Institute of Technology, N.H 44, Hampapuram, Rapthadu, Andhra Pradesh, India*

---

**Abstract** – *Due to their exceptional mechanical characteristics, including effective load distribution and high strength-to-weight ratio, honeycomb structures are extensively employed in a wide range of engineering applications. These structures mirror natural designs, serving as models for the development of robust yet lightweight materials. Inspired by the vascular plant Equisetum, this experimental study examines six unique honeycomb structure configurations to comprehend their mechanical behavior under axial compressive loads. Using PETG reinforced with 0.5% MWCNT material, the structures were created via the Fused Deposition Modelling (FDM) technique. The axial compression behavior of these configurations was experimentally investigated to evaluate variations in mechanical performance across different geometries, highlighting the influence of structural design. The results demonstrated that the H1, H2, and H3 structures outperformed the others, indicating that structural design significantly impacts load distribution, stiffness, and resistance to compressive forces. These findings underscore the potential for optimizing honeycomb structures in engineering applications through careful design, enhancing their already impressive mechanical properties.*

***Key Words***: Honeycomb structures, Axial Compression, Stiffness, Fused Deposition Modelling, PETG, MWCNT

## 1. INTRODUCTION

Recently, honeycomb structures have been renowned for their low strength-to-weight ratio and exceptional energy absorption capabilities, making them a popular choice among researchers for their mechanical properties and acoustic and thermal behaviors [1-2]. However, their evolution continues, drawing inspiration from nature and making them increasingly suitable for diverse engineering applications. Since the 1990s, researchers have played a pivotal role in this ongoing process, exploring innovative designs and materials to enhance the performance of honeycomb structures [3-5]. Research on the optimization of structures with various configurations, including square, circular, triangle, and hierarchical structures, under axial loading conditions, has been extensively documented [6-7]. Recent studies further indicate that small adjustments to the designs of lightweight and high-strength materials can significantly enhance crushing force [8-9]. Similarly, increasing the inward corners of lightweight structures has been shown to improve their energy absorption capacity [10]. Additionally, incorporating corners into the cross-section of tubes has demonstrated a notable improvement in absorption capacity results [11]. Numerous researchers have highlighted that the geometrical changes are crucial for improving the energy absorption capabilities of these structures. This ongoing research underscores the importance of design optimization in enhancing the mechanical performance of materials used in engineering applications. However, studies under different loading conditions, such as tensile, compression, and buckling, have been conducted over the past decades to understand the mechanical properties of these structures [12]. Honeycomb structures have shown superior mechanical characteristics, as evidenced by numerous numerical, experimental, and empirical studies [13]. This ongoing research underscores the importance of design optimization in enhancing the mechanical performance of materials used in engineering applications.

Therefore, in this study, the six bio-inspired honeycomb structures were designed with different configurations that vary with different cell sizes and thicknesses. Where the structures inspired by the vascular plant Equisetum replicated and few changes in geometries were implemented based on the literature. Additionally, a plane hollow cylindrical structure was designed to understand the influence of structural design. Then all different configurations were 3D Printed and subjected to axial compression loading conditions to understand their mechanical behavior. The conclusions were drawn according to the results and discussions were reported.

## 2. MATERIALS AND METHODS

The methodology for developing bioinspired honeycomb structures commenced with the conceptualization and design of these structures, which were inspired by the

vascular systems of plants. These designs were refined and modified based on a thorough literature review to enhance their functionality and structural integrity. Using CAD software, the finalized designs were created in digital form. These digital models were then processed in Ultimaker Cura software and sliced and prepared for 3D printing. Initial tensile tests were conducted on 3D-printed specimens to ensure the desired quality and mechanical strength, thereby validating the printing parameters. Following this validation, the honeycomb structures were consistently printed with the established parameters. Subsequently, compression tests were performed on all seven different honeycomb structures. The results from these tests were meticulously analyzed to evaluate and compare their mechanical performance, thereby providing insights into the effectiveness and potential applications of these bioinspired designs. The methodology followed is depicted in the Figure.

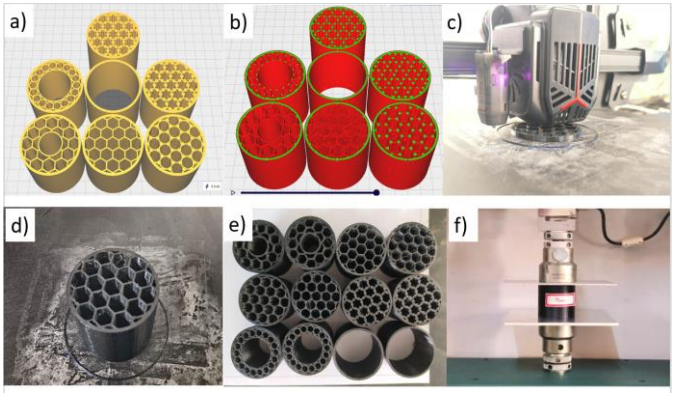


**Fig -1**: Methodology of this study a) CAD Models b)CAD models after Slicing and G-Code generation c) 3D printer representing the specimen preparation d) Output of the 3D-printed Specimen e) Specimens fabricated f) Axial Compression test performed on all the specimens.

## 2.1 Structural design

To design energy absorption column structures in this study six different configurations of honeycomb cells and a plane cylindrical structure were chosen. The same external dimensions were maintained for all specimens. Initially, basic hexagonal unit cells were distributed throughout the structure with a wall thickness of 1 mm and named after H5. The H4 structure was designed to reduce the sharp edges that join at each end of the hexagonal unit cell to the adjacent cell via cylindrical cells of 1.5mm diameter each. Similarly, the structure H2 inculcates cylindrical cells of 1.5mm diameter on every edge of the honeycomb cells. Further, the cylindrical cells were inserted at the edges, vertices, and joints of each honeycomb cell in the H1 structure. The cells consisting the cylindrical cells were prone to eliminate the sharp edges and provided a higher relative density thus resulting in equal load-sharing ability. The H6 structure similar to the H5 had an additional hollow structure at the center resulting in the reduction of relative density. The material at the center was further removed from the center and a circular array of the hexagonal cells were distributed along the inner diameter.

Each structure was inspired by the vascular plant hexagonal cell distribution and the designs with similar geometries with few additional changes according to the literature were inculcated. Finally, their variation in relative density with a lesser number of sharp edges and circular cells provided to absorb and distribute the load applied along axial directions will play a key role in structural integrity.

All bio-inspired hexagonal structures were designed with a cell wall thickness of 1mm, 46 mm as the inner diameter of the cylinder, outer diameter of 50mm, and height was 50mm for all structures i.e., H1, H2, H3, H4, H5, H6, and H7. The plain cylindrical hollow structure was designed to compare performance over the honeycomb cell structures with higher relative density. Based on the literature, a few sharp edges and geometrical changes were done to honeycomb unit cells to improve the energy absorption capabilities. Figure 2 represents the dimensions chosen and their top views.

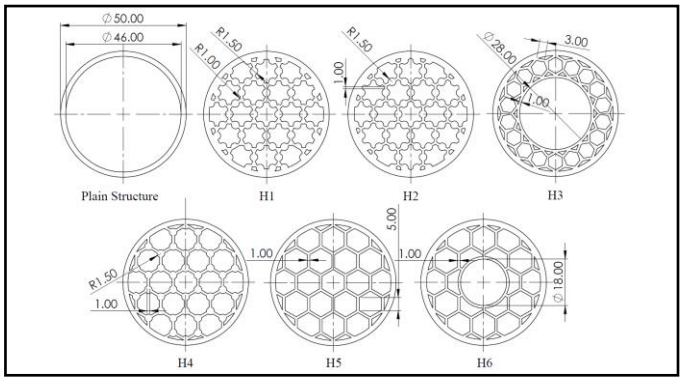


**Fig -2**: Structural designs and dimensions of different honeycomb structures

## 2.2 Materials

PETG, a thermoplastic material known for its high impact resistance and ductility, is widely used in Fused Deposition Modeling (FDM) due to its ease of printing and versatility [14]. The addition of MWCNTs to PETG has been shown to further enhance its mechanical, thermal, and tribological properties while maintaining its versatility and printing quality [15]. PETG composite material has been chosen in this study, due to the low amount of shrinkage and odorless printing with 100 % recyclability.

PETG MWCNT filament of 1.75 mm diameter had been procured from Rever Industries - Mumbai. The PETG had 99.5% of the volume content and MWCNT had 0.5% of the volume content throughout the filament. The density of the PETG 0.5% MWCNT composite filament is $\rho$ = 1.25 g/cm$^3$.

### 2.3 Fabrication through FDM

In recent years, Fused Deposition Modeling (FDM) has evolved significantly to become the core of additive manufacturing because of its adaptability, affordability, and high degree of precision in creating complex geometries.[16] The range of applications for FDM has increased with the introduction of different thermoplastics, metal-infused filaments, and especially composites. This has made it possible to produce functional parts with improved mechanical properties. Due to these advancements, FDM is now a well-liked option in preparation of the energy absorption structures seamlessly where producing durable, customized components quickly and efficiently is crucial.[17].

The FDM with appropriate printing parameters for the chosen material and perfect infill patterns can result in high-quality components with better mechanical properties. PETG 0.5%MWCNT has a glass transition temperature of 75°c and a Melting temperature of 240 °c. So, the nozzle temperature was chosen to be 245 °c and the bed temperature was 80°c. The samples were printed at room temperature. The steel nozzle with 0.4mm diameter was chosen for printing due to the advantages such as higher wear resistance, temperature resistance, and low clogging over the brass nozzle. The samples are designed in CAD software under ASTM-695 standards and printed in the WOL 3D Printer procured from Creality. The Ultimaker-Cura software had been utilized for slicing operations. The printing parameters are given in Table 1.

**Table -1:** Printing parameters utilized in this study

| SI No | Parameters | PETG 0.5% MWCNT |
|---|---|---|
| 1 | Infill density | 100% |
| 2 | Nozzle Temperature | 230 |
| 3 | Build platform temperature | 75 |
| 4 | Printing speed | 35mm/min |
| 5 | Raster angle | +45/-45◦ |
| 6 | First layer height | 0.3 mm |
| 7 | Layer height | 0.2 mm |

### 2.4 Mechanical Characterization

The fabricated structures were subjected to mechanical characterization tests to understand the behaviors under tensile and compression loading. The tensile tests were performed according to the ASTM D-638 Type-V standards and ASTM 690 standards for compression testing at room temperature. For repeatability, three specimens for each configuration of structures were tested and the average values were finalized and reported. The tensile tests were performed on the Universal Testing Machine (Instron 10KN load cell) at a constant strain rate of 2mm/min and stress vs strain plots were obtained. And, compression tests were also performed at a constant strain rate of 2mm/min. The tests were terminated when the densification stage was observed while axial compression loads were applied. Then force vs displacement plots were obtained from the test results to understand their deformation behavior. The tensile samples had the dimensions of 63.5 x 9.53 x 3.2mm and compression test samples had 50mm diameter x 50mm dimensions.

## 3. Results and Discussions

### 3.1 Tensile Characterization

Tensile tests were performed to obtain the tensile strength and to understand the failure criterion. Through visual inspection, it is evident that the tensile specimen at the gauge length was elongated and the polymer chains were elongated along the tensile load direction. The elongation with an increase in the tensile strength was continued until it reached to ultimate tensile strength of 45.5 MPa, and then neck growth was stopped. Then, the elongation was continued at a slower rate with decreased strain until the crack propagated was ended up with a specimen break. From the results shown in Figure 2, the displacement initially in the elastic region increased at a very slow rate with an increase in the tensile strength. When the tensile strength dropped a bit to MPa and constant increase was noticed in the necking region. The maximum recorded strain was 18 mm.

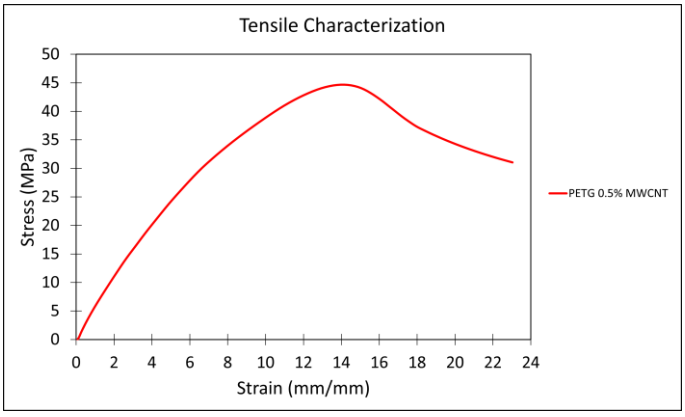


**Fig -2**: Stress vs Strain Plot obtained from the tensile test on PETG 0.5% MWCNT sample

However, the 3d printed layers along the direction of the print tended to support and resist the specimen to failure. From the results of the stress-strain plot, it is evident that the specimens have undergone elongation, followed by necking and thinning.

The results represented in the figure, indicate the UTS was 45.5 MPa and the interlayer bonding was stronger

among 3D printed specimens. Likely, the 3D printing parameters chosen had given the better output which concluded the parameters followed will get appropriate results and thus, a similar procedure had been followed in 3D printing all the honeycomb configurations.

### 3.1 Compression Characterization

The compression tests for plane cylindrical and all honeycomb configurations were performed at a constant strain rate and their results were presented. The results include the force vs displacement plots obtained under the axial compression loading at 2mm/min shown in Figure 3. Further, the load absorbed and displacements obtained were plotted individually for each specimen represented in Figure 4 and Figure 5.

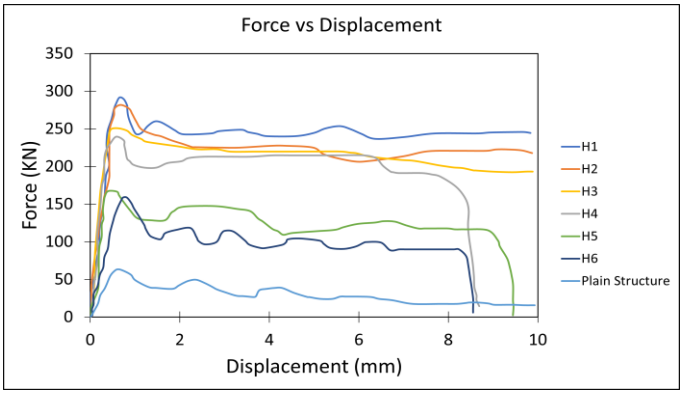


**Fig -3**: Force vs Displacement for all structures

Initially, the plane cylindrical structure was subjected to the axial load on its top surface and the maximum load obtained was 63.38 KN with a maximum displacement of 10 mm. The top surface subjected to load started to absorb the load until it gradually reached 63 KN, then it started to exhibit nonlinearity and ended up with a buckle on the loaded end resulting the fluctuations in the force vs displacement plots. During buckling, an instability compression was observed due to the sudden phase changes between the hard and soft phases within the structure of the material.

The H1 structure was able to withstand the maximum load of 291.55 KN compared to all honeycomb structural configurations and obtained a displacement of 9.78 mm. The H1 structure exhibited higher load bearing capacity which was 78.26% higher than the conventional plane cylindrical structure. Due to its higher relative density and cylindrical cells, with minimal sharp edges resulted in the reduction of stress concentration and proper load distribution throughout the structure. The Samples were buckled at the top end where the axial load was applied. After the maximum load was attained, the structure started to buckle along the edges of the cylindrical walls.

Similar to structure H1, the same buckling pattern was obtained at the contact of cylindrical walls to the unit cells and also at contacts among the unit cells. Due to the absence of cylindrical cells at the edges, the resistance to load was reduced when compared to structure H1. However, structure H2 with 77.9% higher load-bearing capacity than the plane cylindrical structure and ended up with densification at the maximum displacement of 9.87mm.

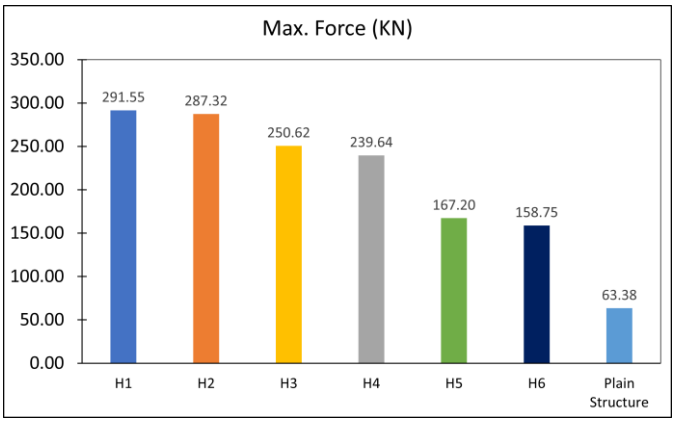


**Fig -4**: Maximum Force in KN obtained under axial compression test for all structures

Structure H4 exhibited a similar way of buckling to H2 where the cracks were propagated from the vertices of the unit cells to edges and contacts between the unit cells to the outer cylindrical wall of the structure. However, the structure H4 exhibited lower load-bearing capacity when compared to H1, H2, and H3 and 73.55% higher than the plane cylindrical structure.

The structure H3 has exhibited better resistance to applied load when compared to H4, H5, and H6 structures. Unlike the H1 and H2 structures H3 consists of a hollow inner wall and its cells are distributed in a circular array. Due to its unique cell distribution, its relative density was higher which helps in resisting the sudden collapse of structure under axial loading. Even though the unit cell collapsing was initiated at the center of the structure on the inner wall to unit cell contact it propagated eventually ending up with buckling. However, compared to the plane cylindrical structure it was able to exhibit 74.71% higher load-bearing capacity.

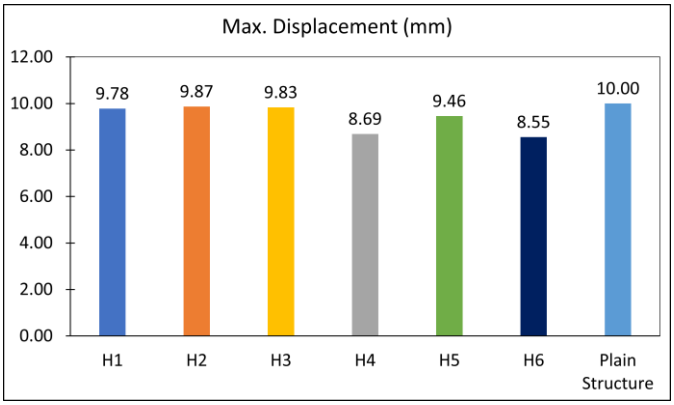


**Fig -4**: Maximum Displacement in mm obtained under axial compression test for all structures

The structure H5 consists of evenly distributed honeycomb cells which led to exhibiting better load-bearing capability, which was 62% higher than the conventional plane cylindrical structure. The structure was buckled along the contacts of unit cells with the inner walls of the outer cylindrical structure. The maximum load obtained from the results was 167.20 KN.

The structure H6 exhibited a 60% higher load-bearing capacity than the conventional plane cylindrical structure. The collapse of the unit cells initiated at the inner walls and propagated to the unit cells and eventually ended up with the buckling failure at 158.75 KN.

## 4. CONCLUSIONS

In this study, the mechanical characterization and deformation behavior of the plane cylindrical, H1, H2, H3, H4, H5, and H6 hexagonal structures under axial compression load were investigated. The hexagonal structures were designed after vascular plant hexagonal cell distribution, with few additional changes according to the literature. These structures were 3D Printed through the FDM technique and subjected to axial compression loads under ASTM standards at room temperature.

From the results, it was observed that the changes in structural topology at a gradual level were influencing the mechanical performance of honeycomb structures. In addition, the circular unit cells were able to reduce the stress concentrations when inculcated at edges, vertices, and joints between unit cells. All structures showed distinct deformation behaviors based on their relative density and geometrical stiffness when subjected to axial loading. However, they exhibited similar failures beginning with geometrical nonlinearity during loading at the top surface of each structure resulting the fluctuations in force vs displacement plots. Then break of contact of the unit cells with walls and contact in between unit cells gradually starts collapsing when entered into to softening phase and offers resistance when they are in the hardening phase. Ultimately, the irregular pattern in the force vs displacement plot was continued until the structures ended up buckling. However, when compared to plain conventional cylindrical structure the H1 structure showed 78.26%, the H2 structure 77.9 %, the H3 structure 74.71%, the H4 structure 73.55 %, the H5 structure 62%, and the H6 structure 60% increased load bearing capacities.

## REFERENCES

[1] Gao, Nansha, Hong Hou, and Jiu Hui %J International Journal of Modern Physics B Wu. 2018. "A composite and deformable honeycomb acoustic metamaterial.", 32 (20):1850204.

[2] Almutairi, Mohamed M, Mohamed Osman, and Iskander %J Journal of Energy Resources Technology Tlili. 2018. "Thermal behavior of auxetic honeycomb structure: an experimental and modeling investigation." 140 (12):122904.

[3] Bitzer, Tom. 1997. "Honeycomb core." In *Honeycomb Technology: Materials, Design, Manufacturing, Applications and Testing*, 10-42. Springer.

[4] Xiang, Jinwu, Jianxun %J Materials Science Du, and Engineering: A. 2017. "Energy absorption characteristics of bio-inspired honeycomb structure under axial impact loading." 696:283-289.

[5] Chen, BC, M Zou, GM Liu, JF Song, and HX %J International Journal of Impact Engineering Wang. 2018. "Experimental study on energy absorption of bionic tubes inspired by bamboo structures under axial crushing." 115:48-57.

[6] Smeets, Bart JR, Edward M Fagan, Kelly Matthews, Robert Telford, Brendan R Murray, Leonid Pavlov, Bryan Weafer, Patrick Meier, and Jamie %J Composites Part B: Engineering Goggins. 2021. "Structural testing of a shear web attachment point on a composite lattice cylinder for aerospace applications." 212:108691.

[7] Sun, Guangyong, Xintao Huo, Hongxu Wang, Paul J Hazell, and Qing %J Composites Part B: Engineering Li. 2021. "On the structural parameters of honeycomb-core sandwich panels against low-velocity impact." 216:108881.

[8] San Ha, Ngoc, and Guoxing %J Composites Part B: Engineering Lu. 2020. "A review of recent research on bio-inspired structures and materials for energy absorption applications." 181:107496.

[9] McKittrick, J, P-Y Chen, L Tombolato, EE Novitskaya, MW Trim, GA Hirata, EA Olevsky, MF Horstemeyer, MA %J Materials Science Meyers, and Engineering: C. 2010.

"Energy absorbent natural materials and bioinspired design strategies: a review." 30 (3):331-342.

[10] Zhang, Jianjun, Guoxing Lu, and Zhong %J Composites Part B: Engineering You. 2020. "Large deformation and energy absorption of additively manufactured auxetic materials and structures: A review." 201:108340.

[11] Zahran, MS, Pu Xue, and MS %J International Journal of Crashworthiness Esa. 2017. "Novel approach for design of 3D-multi-cell thin-walled circular tube to improve the energy absorption characteristics under axial impact loading." 22 (3):294-306.

[12] Xu, Mengchuan, Ziran Xu, Zhong Zhang, Hongshuai Lei, Yingchun Bai, and Daining %J International Journal of Mechanical Sciences Fang. 2019. "Mechanical properties and energy absorption capability of AuxHex structure under in-plane compression: Theoretical and experimental studies." 159:43-57.

[13] Alhat, Sumeet M, and Manisha H Yadav. 2020. "Mechanical and Electrical Behavior of Polyethylene Terephthalate Glycol (PETG) Reinforced with Multiwall Carbon Nanotubes (MWCNT) by using Fused Deposition Modeling 3D Printing."

[14] Özen, Arda, Bilen Emek Abali, Christina Völlmecke, Jonathan Gerstel, and Dietmar %J Applied Composite Materials Auhl. 2021. "Exploring the role of manufacturing parameters on microstructure and mechanical properties in fused deposition modeling (FDM) using PETG." 28 (6):1799-1828.

[15] Solomon, I John, P Sevvel, and JJMTP %J Materials Today: Proceedings Gunasekaran. 2021. "A review on the various processing parameters in FDM." 37:509-514.

[16] Sankineni, Rakesh, and Y %J Proceedings of the Institution of Mechanical Engineers Ravi Kumar, Part C: Journal of Mechanical Engineering Science. 2022. "Evaluation of energy absorption capabilities and mechanical properties in FDM printed PLA TPMS structures." 236 (7):3558-3577.

[17] Zurnacı, Erman, and Haydar Kadir %J Gazi Mühendislik Bilimleri Dergisi Özdemir. 2023. "Investigation of the compressive strength, energy absorption properties and deformation modes of the reinforced core cell produced by the FDM method." 9 (1):1-11.